PHASE 2 INITIAL BOREHOLE DRILLING AND TESTING, IGNACE AREA

WP10: Rock Mass Classification for IG_BH04, IG_BH05, and IG_BH06

APM-REP-01332-0283 **October 2024**

WSP Canada Inc.

nwmo
NUCLEAR WASTE MANAGEMENT ORGANIZATION
SOCIÉTÉ DE GESTION DES DÉCHETS NUCLÉAIRES

This report has been prepared under contract to NWMO. The report has been reviewed by NWMO, but the views and conclusions are those of the authors and do not necessarily represent those of the NWMO.

All copyright and intellectual property rights belong to NWMO.

Nuclear Waste Management Organization
22 St. Clair Avenue East, 4th Floor
Toronto, Ontario
M4T 2S3
Canada

Tel: 416-934-9814
Web: www.nwmo.ca

REPORT

PHASE 2 INITIAL BOREHOLE DRILLING AND TESTING AT IG_BH04/05/06, IGNACE AREA

WP10 - Rock Mass Classification for IG_BH04, IG_BH05, and IG_BH06

Submitted to:

Nuclear Waste Management Organization

4th Floor
22 St. Clair Avenue East
Toronto, Ontario, M4T 2S3

Submitted by:

WSP Canada Inc.

6925 Century Avenue, Suite #600, Mississauga, Ontario, L5N 7K2, Canada

+1 905 567 4444

20253946 (4100/5100/6100)

NWMO Report: APM-REP-01332-0283

October 2024

Distribution List

NWMO - 1 eCopy

WSP Canada Inc. - 1 eCopy

WP10 REPORT – ROCK MASS CLASSIFICATION FOR IG_BH04, IG_BH05, AND IG_BH06

CLIENT INFORMATION

Project Name:	Phase 2 Initial Borehole Drilling and Testing - Ignace Area
Project Number:	20253946
Client PO Number:	2001102
Document Name:	20253946_rpt_wp10_rmr_for_ig_bh04_05_06_r4a

Client:	Nuclear Waste Management Organization (NWMO)
Address:	22 St. Clair Avenue East, Fourth Floor
City:	Toronto
Province:	Ontario
Postal Code:	M4T 2S3
Client Contact:	Aaron DesRoches and Warwick Watt
Telephone:	437-972-3669 437-972-3669
Email:	adesroches@nwmo.ca and wwatt@nwmo.ca

ISSUE/REVISION INDEX

Issue Code	Revision					Revision Details
	No.	By	Rev'd.	App.	Date	
RR	0	JLC	IL	GWS	December 15, 2023	Draft for review and comments
RR	1	JLC	IL	GWS	April 03, 2024	Draft for review and comments
RI	2	JLC	IL	GWS	May 15, 2024	Final released for information
RI	3	JLC	IL	GWS	September 18, 2024	Final released for information
RI	4	JLC	IL	GWS	October 04, 2024	Final released for information

Issue Codes: RR = Released for Review and Comments, RI = Released for Information

SIGNATURES

Prepared by: _____

Joe Carvalho, Ph.D., P.Eng.
Mining & Rock Engineering – Fellow

Reviewed by: _____

Iris Lenauer, Ph.D., P.Geo.
Mining & Rock Engineering Group

Approved by: _____

George Schneider, M.Sc., P.Geo.
Senior Geoscientist – Fellow

Table of Contents

1.0 INTRODUCTION 1

2.0 BACKGROUND INFORMATION 1

2.1 Geological Setting 1

3.0 OBJECTIVE 6

4.0 FINAL STRUCTURE LOG 6

5.0 GEOMECHANICS CLASSIFICATION, ROCK MASS RATING (RMR) INDEX 12

6.0 SUMMARY OF ROCK MASS CLASSIFICATION PARAMETERS 14

6.1 Strength 14

6.1.1 IG_BH04 14

6.1.2 IG_BH05 14

6.1.3 IG_BH06 15

6.2 RQD 16

6.2.1 IG_BH04 16

6.2.2 IG_BH05 16

6.2.3 IG_BH06 16

6.3 Fracture Spacing 16

6.3.1 IG_BH04 16

6.3.2 IG_BH05 17

6.3.3 IG_BH06 17

6.4 Condition of Discontinuities 17

6.4.1 IG_BH04 17

6.4.2 IG_BH05 18

6.4.3 IG_BH06 18

6.5 Groundwater 19

6.5.1 IG_BH04 19

6.5.2 IG_BH05 19

6.5.3 IG_BH06 20

7.0 SUMMARY OF ROCK MASS CLASSIFICATION BY RUN 20

8.0 SUMMARY OF ROCK MASS RATING INDEX DISTRIBUTION BY SECTIONS OF BOREHOLE IG_BH04, IG_BH05, AND IG_BH06 25

8.1 Adjustments to RMR Data for Engineering Use 25

8.1.1 Groundwater Ratings 25

8.1.2 Rating Adjustments for Discontinuity Orientations 25

9.0 REFERENCES 30

TABLES

Table 1: Example of Integrated Structure Log Compilation 8

Table 2: Rock Mass Rating System (Geomechanics Classification of Rock Masses, Bieniawski (1989)) 13

Table 3: UCS Values and Locations of Samples for IG_BH04, IG_BH05 and IG_BH06 15

Table 4: Summary of Hydraulically Conductive Feature Intervals for IG_BH04 19

Table 5: Summary of Hydraulically Conductive Feature Intervals for IG_BH05 20

Table 6: Summary of Hydraulically Conductive Feature Intervals for IG_BH06 20

Table 7: Summary of Mean and Median Values for RMR Index for IG_BH04, IG_BH05 and IG_BH06 25

Table 8: Rating Adjustment for Discontinuity Orientations (see also Table 9) 26

Table 9: Effect of Discontinuity Strike and Dip on Orientation in Tunnelling 26

FIGURES

Figure 1: Location of Boreholes in Relation to the Ignace Area 4

Figure 2: Geological Setting and Location of Boreholes IG_BH04, IG_BH05, and IG_BH06 in the Northern Portion of the Revell Batholith 5

Figure 3: Stereographic Projection of all Integrated Structures for IG_BH04: Top: Structures by Type; Bottom: Contour Plot (with Terzaghi Weighting) 9

Figure 4: Stereographic Projection of all Integrated Structures for IG_BH05: Top: Structures by Type; Bottom: Contour Plot (with Terzaghi Weighting) 10

Figure 5: Stereographic Projection of all Integrated Structures for IG_BH06: Top: Structures by Type; Bottom: Contour Plot (with Terzaghi Weighting) 11

Figure 6: Summary Profile of Rock Mass Characteristics, Including Components of RMR'89, Used to Develop the RMR Index (Rightmost Column) for IG_BH04 22

Figure 7: Summary Profile of Rock Mass Characteristics, Including Components of RMR'89, Used to Develop the RMR Index (Rightmost Column) for IG_BH05 23

Figure 8: Summary Profile of Rock Mass Characteristics, Including Components of RMR'89, Used to Develop the RMR Index (Rightmost Column) for IG_BH06 24

Figure 9: RMR Index Distribution for 100 m Sections of Borehole (RMR Index by Run) for IG_BH04 27

Figure 10: RMR Index Distribution for 100 m Sections of Borehole (RMR Index by Run) for IG_BH05 28

Figure 11: RMR Index Distribution for 100 m Sections of Borehole (RMR Index by Run) for IG_BH06 29

1.0 INTRODUCTION

The Phase 2 Initial Borehole Drilling and Testing at IG_BH04/05/06 project in the Wabigoon Lake Ojibway Nation (WLON) – Ignace area of Ontario, is part of the Phase 2 Geoscientific Preliminary Field Investigations of the Nuclear Waste Management Organization's (NWMO) Adaptive Phased Management (APM) Site Selection Phase.

This project involves the drilling and testing of deep boreholes IG_BH04, IG_BH05 and IG_BH06 in the Revell Site within the identified Potential Repository Area (PRA). The boreholes are located a direct distance of approximately 23 km southeast of the Wabigoon Lake Ojibway Nation and a direct distance of 42 km northwest of the Town of Ignace. Access to the drill sites is via Highway 17 and primary logging roads, as shown on Figure 1. The work comprised of a total of eleven work packages and was carried out by a team led by Golder Associates Ltd. (now WSP Canada Inc.) on behalf of the NWMO. The programs for IG_BH04, IG_BH05 and IG_BH06 are described in the Borehole Characterization Plans.

This report describes the rock mass classification based on the data collected during the field activities for borehole IG_BH04 by Wood, and IG_BH05 and IG_BH06 by WSP, and the subsequent analyses and compilation of the data (e.g., borehole logs, laboratory testing and hydrogeology), as described in the work plans of WP03 – Geological and Geotechnical Core Logging, Photography and Sampling, WP10 – Final Structure Log, WP03-WP05-WP07 Integrated dataset – Hydraulically Conductive Features, and core testing (WP04B - Geomechanics) for IG_BH04, IG_BH05 and IG_BH06.

2.0 BACKGROUND INFORMATION

2.1 Geological Setting

The approximately 2.7 billion year old Revell batholith is located in the western part of the Wabigoon Subprovince of the Archean Superior Province. The batholith is roughly elliptical in shape trending northwest, is approximately 40 km in length, 15 km in width, and covers an area of approximately 455 km^2. Based on geophysical modelling, the batholith is approximately 2 km to 3 km thick through the center of the northern portion (SGL 2015). The batholith is surrounded by supracrustal rocks of the Raleigh Lake (to the north and east) and Bending Lake (to the southwest) greenstone belts (Figure 2).

The boreholes are located in the northern portion of the Revell batholith. Bedrock exposure in the area is generally very good due to minimal overburden, few water bodies, and relatively recent logging activities. Ground elevations generally range from 400 to 450 m above sea level. The ground surface broadly slopes towards the northwest as indicated by the flow direction of the main rivers in the area. Local water courses tend to flow to the southwest towards Mennin Lake (Figure 1).

Four main rock units are identified in the supracrustal rock group: mafic metavolcanic rocks, intermediate to felsic metavolcanic rocks, metasedimentary rocks, and mafic intrusive rocks (Figure 2). Sedimentation within the supracrustal rock assemblage was largely synvolcanic, although sediment deposition in the Bending Lake area may have continued past the volcanic period (Stone 2009; Stone 2010a; Stone 2010b). All supracrustal rocks are affected, to varying degrees, by penetrative brittle-ductile to ductile deformation under greenschist- to amphibolite-facies metamorphic conditions (Blackburn and Hinz 1996; Stone et al. 1998). In some locations, primary features, such as pillow basalt or bedding in sedimentary rocks are preserved; in other locations, primary relationships are completely masked by penetrative deformation. Uranium-lead (U-Pb) geochronological analysis of the supracrustal rocks produced ages that range between 2734.6 +/-1.1 Ma and 2725 +/-5 Ma (Stone et al. 2010).

Three main suites of plutonic rock are recognized in the Revell batholith, including, from oldest to youngest: a Biotite Tonalite to Granodiorite suite, a Hornblende Tonalite to Granodiorite suite, and a Biotite Granite to Granodiorite suite (Figure 2). Plutonic rocks of the Biotite Tonalite to Granodiorite suite occur along the southwestern and northeastern margins of the Revell batholith. The principal type of rock within this suite is a white to grey, medium-grained, variably massive to foliated or weakly gneissic, biotite tonalite to granodiorite. One sample of foliated and medium-grained biotite tonalite produced a U-Pb age of 2734.2+/-0.8 Ma (Stone et al. 2010). The Hornblende Tonalite to Granodiorite suite occurs in two irregularly-shaped zones surrounding the central core of the Revell batholith. Rocks of the Hornblende Tonalite to Granodiorite suite range compositionally from tonalite through granodiorite to granite and also include significant proportions of quartz diorite and quartz monzodiorite. One sample of coarse-grained grey mesocratic hornblende tonalite produced a U-Pb age of 2732.3+/-0.8 Ma (Stone et al. 2010). Rocks of the Biotite Granite to Granodiorite suite underlie most of the northern, central and southern portions of the Revell batholith. Rocks of this suite are typically coarse-grained, massive to weakly foliated, and white to pink in colour. The Biotite Granite to Granodiorite suite ranges compositionally from granite through granodiorite to tonalite. A distinct potassium (K)-Feldspar Megacrystic Granite phase of the Biotite Granite to Granodiorite suite occurs as an oval-shaped body in the central portion of the Revell batholith (Figure 2). One sample of coarse-grained, pink, massive K-feldspar megacrystic biotite granite produced a U-Pb age of 2694.0+/-0.9 Ma (Stone et al. 2010).

The bedrock surrounding IG_BH04, IG_BH05, and IG_BH06 is composed mainly of massive to weakly foliated felsic intrusive rocks that vary in composition between granodiorite and tonalite, and together form a relatively homogeneous intrusive complex. Bedrock identified as tonalite transitions gradationally into granodiorite and no distinct contact relationships between these two rock types are typically observed (SRK and Golder 2015; Golder and PGW 2017). Massive to weakly foliated granite is identified at the ground surface to the northwest of the feldspar-megacrystic granite. The granite is observed to intrude into the granodiorite-tonalite bedrock, indicating it is distinct from, and younger than, the intrusive complex (Golder and PGW 2017).

West-northwest trending mafic dykes interpreted from aeromagnetic data extend across the northern portion of the Revell batholith and into the surrounding greenstone belts. One mafic dyke occurrence, located to the northwest of IG_BH01, is approximately 15-20 m wide (Figure 2). All of these mafic dykes have a similar character and are interpreted to be part of the Wabigoon dyke swarm. One sample from the same Wabigoon swarm produced a U-Pb age of 1887+/-13 Ma (Stone et al. 2010), indicating that these mafic dykes are Proterozoic in age. It is assumed based on surface measurements that these mafic dykes are sub-vertical (Golder and PGW 2017).

Long, narrow valleys are located along the western and southern limits of the investigation area (Figure 1). These local valleys host creeks and small lakes that drain to the southwest and may represent the surface expression of structural features that extend into the bedrock. A broad valley is located along the eastern limits of the investigation area and hosts a more continuous, un-named water body that flows to the south. The linear and segmented nature of this waterbody's shorelines may also represent the surface expression of structural features that extend into the bedrock.

Regional observations from mapping have indicated that structural features are widely spaced (typical 30 to 500 cm spacing range) and dominantly comprised of sub-vertical joints with two dominant orientations, northeast and northwest trending (Golder and PGW 2017). Interpreted bedrock lineaments generally follow these same dominant orientations in the northern portion of the Revell batholith (Figure 2; DesRoches et al. 2018). Minor sub-horizontal joints have been observed with minimal alteration, suggesting they are younger and perhaps related to

glacial unloading. One mapped regional-scale fault, the Washeibemaga Lake fault, trends east and is located to the west of the Revell batholith (Figure 2). Fabric-concordant lineaments, also shown on Figure 2, follow the trend of foliation mapped in the surrounding greenstone belts. Additional details of the lithological units and structures found at surface within the investigation area are reported in Golder and PGW (2017).

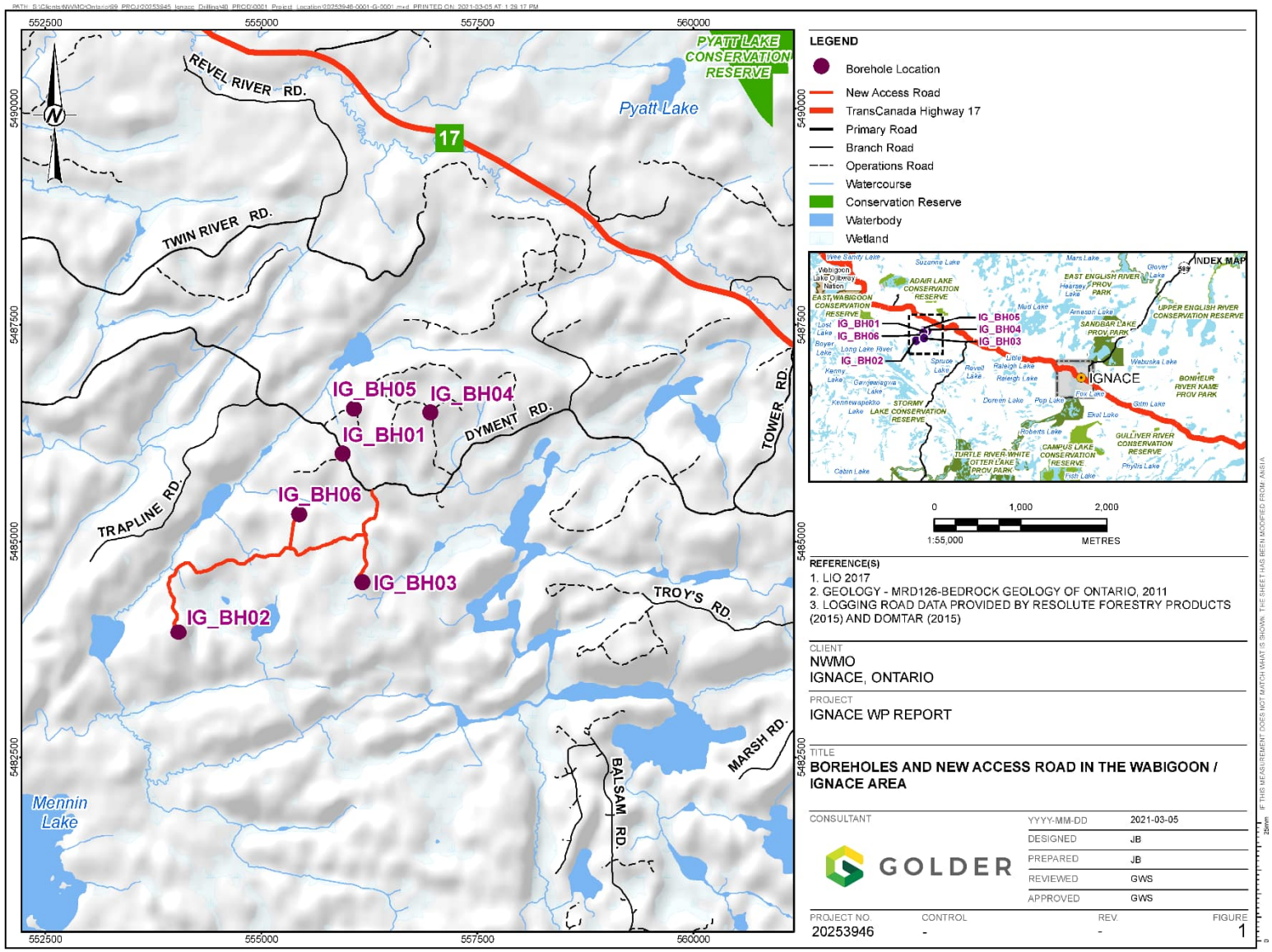


Figure 1: Location of Boreholes in Relation to the Ignace Area

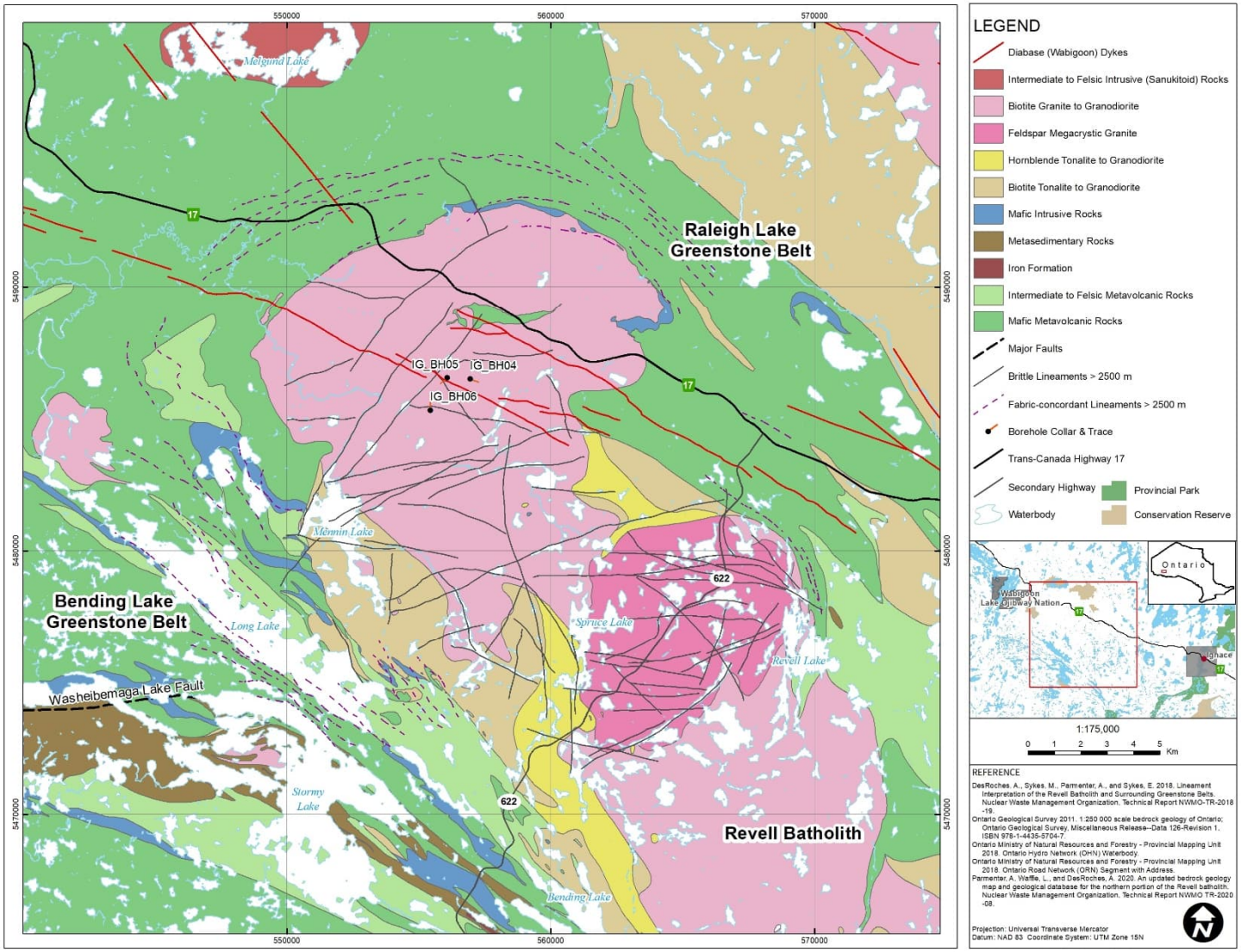


Figure 2: Geological Setting and Location of Boreholes IG_BH04, IG_BH05, and IG_BH06 in the Northern Portion of the Revell Batholith

3.0 OBJECTIVE

The objective of this report is to present the methodology and the results for the development of the Rock Mass Rating (RMR) Index profile (along borehole) for boreholes IG_BH04, IG_BH05 and IG_BH06. The report also presents a summary of the final structure log developed through the integration of structures identified during core logging, WP03 (Wood 2021, WSP 2023a, 2023b) and downhole televiewer logging, WP05 (WSP 2022a, 2023c, 2023d), which is an important input into the RMR Index presented herein. The final structure log is a part of completion of the WP10 geological integration reports for IG_BH04 (DesRoches et al. 2023), IG_BH05 (Markovic et al. 2024a) and IG_BH06 (Markovic et al. 2024b).

4.0 FINAL STRUCTURE LOG

During drilling of borehole IG_BH04, the orientation of all structures measured during core logging, as described in the WP03 (Wood 2021) data report, are initially defined based on alpha and beta angles relative to (1) the core axis, and (2) a reference line (bottom of the borehole) drawn along the length of each core run, as identified by the Reflex ACT III tool. These orientation angles (alpha/beta for planes; gamma/delta for lineations) for each logged structure were reconciled with the oriented structures identified by the televiewer logs.

During drilling of boreholes IG_BH05 and IG_BH06, the orientation of all structures measured during core logging, as described in the WP03 data reports (WSP 2023a, 2023b), are initially defined based on alpha and beta angles relative to (1) the core axis, and (2) an arbitrary reference line drawn along the length of each core run. Since the core retrieved from the boreholes (IG_BH05 and IG_BH06) is not oriented, these relative orientation angles (beta for planes; delta for lineations) for each logged structure need to be corrected to a true orientation in order to produce the final structure logs. As part of this process, structures were also interpreted by the geophysical team (WP05) using optical and acoustic televiewer logs independently of the structures picked from the core logging. Interpreted structure orientations were corrected from apparent dip and dip direction to true dip and dip direction (i.e., relative to true north), using the final Tilt and Azimuth logs, as described in the WP05 data reports (Golder, 2023d, 2023e).

Once both WP03 and WP05 interpretations were completed, they were integrated as a specific task as part of completion of the WP10 geological integration reports for IG_BH04 (DesRoches et al. 2023), IG_BH05 (Markovic et al. 2024a) and IG_BH06 (Markovic et al. 2024b). This comparison identified structures that are common to both televiewer logs and core logging, based on similar position along borehole and relationship to adjacent structures, and possibly structure type and its characteristics (e.g., geological aperture). The complete methodology used in integrating the structures into a final structure log is included in Appendix D of the WP10 reports (DesRoches et al. 2023; Markovic et al. 2024a, b).

Geological aperture is an estimated measurement of the open space between two adjacent fracture surfaces determined visually during geological core logging, during interpretation of downhole televiewer logs, or during the integration of data from these two sources. For our purposes, geological apertures are estimated values only because there are multiple possible sources of uncertainty in how a reported aperture value relates to the true aperture of a fracture identified as broken. There are uncertainties related to measurement inaccuracy, including where the opening is very small, where the opposing fracture planes are not parallel or fit poorly together, or due to limits in televiewer resolution. In addition, effects due to drilling or decompression may create or enhance the visible open space identified as aperture. Finally, aperture measured in core or on a borehole wall is only a local aperture that is not necessarily representative over the entire fracture.

The result of the integrated structure log includes a table that captures a complete set of attributes of each structure recorded either from core logging, televiewer logging, or a combination of both. Where certain attributes are duplicated between the two logging approaches (i.e., structure type, or position along borehole) decisions are made to carry forward the most accurate value to the final structure log. For example, orientation data will be obtained from the televiewer logged structures, whereas structure type should be obtained from core logging structures. Table 1 shows an example of the integrated structure log compilation. Figure 3 through Figure 5 show stereographic projections of the integrated final structures by type (top) and a contoured plot of all integrated final structures (bottom) for boreholes IG_BH04, IG_BH05, and IG_BH06, respectively.

Table 1: Example of Integrated Structure Log Compilation

Structure #	Reference Line	Beta CF	Beta CF St. Dev.	Final Depth	Corr_ Alpha	Corr_ Beta	True_Dip	True_ DDIR	Type	Condition	Width (cm)	Geological Aperture (mm)	Infill Thickness (mm)
45	RL011	200.40	0.00	6.99	69	175	2	93	JN	BR	-	5	0
49	RL012	263.35	6.03	7.45	62	188	8	214	JN	BR	-	0	0
50	RL012	263.35	6.03	7.51	60	238	25	283	JN	PIN	-	0	0
51	RL012	263.35	6.03	7.52	18	106	68	103	JN	BR	-	1	1
52	RL012	263.35	6.03	7.65	67	233	19	294	JN	PIN	-	0	0
53	RL012	263.35	6.03	8.20	22	317	84	326	JN	BR	-	0	0
54	RL012	263.35	6.03	8.29	17	102	70	100	JN	IN	-	0	1

NOTE:
Beta CF – Beta Correction Factor for the reference line
Beta CF St. Dev. – Standard deviation for Beta Correction Factor for the reference line
Joint – JN
BR – Broken
IN – Intact
PIN – Partially intact

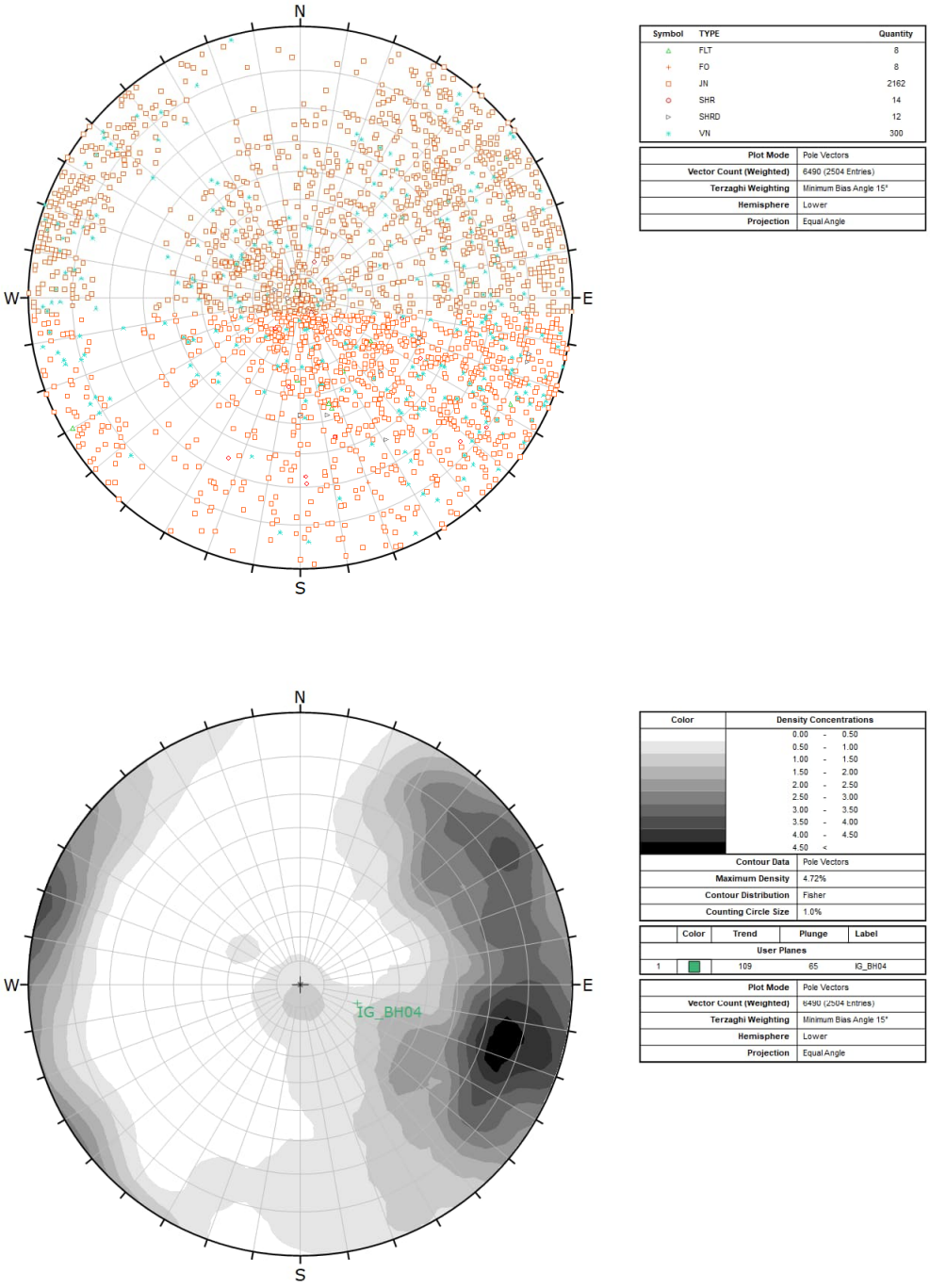


Figure 3: Stereographic Projection of all Integrated Structures for IG_BH04: Top: Structures by Type; Bottom: Contour Plot (with Terzaghi Weighting)

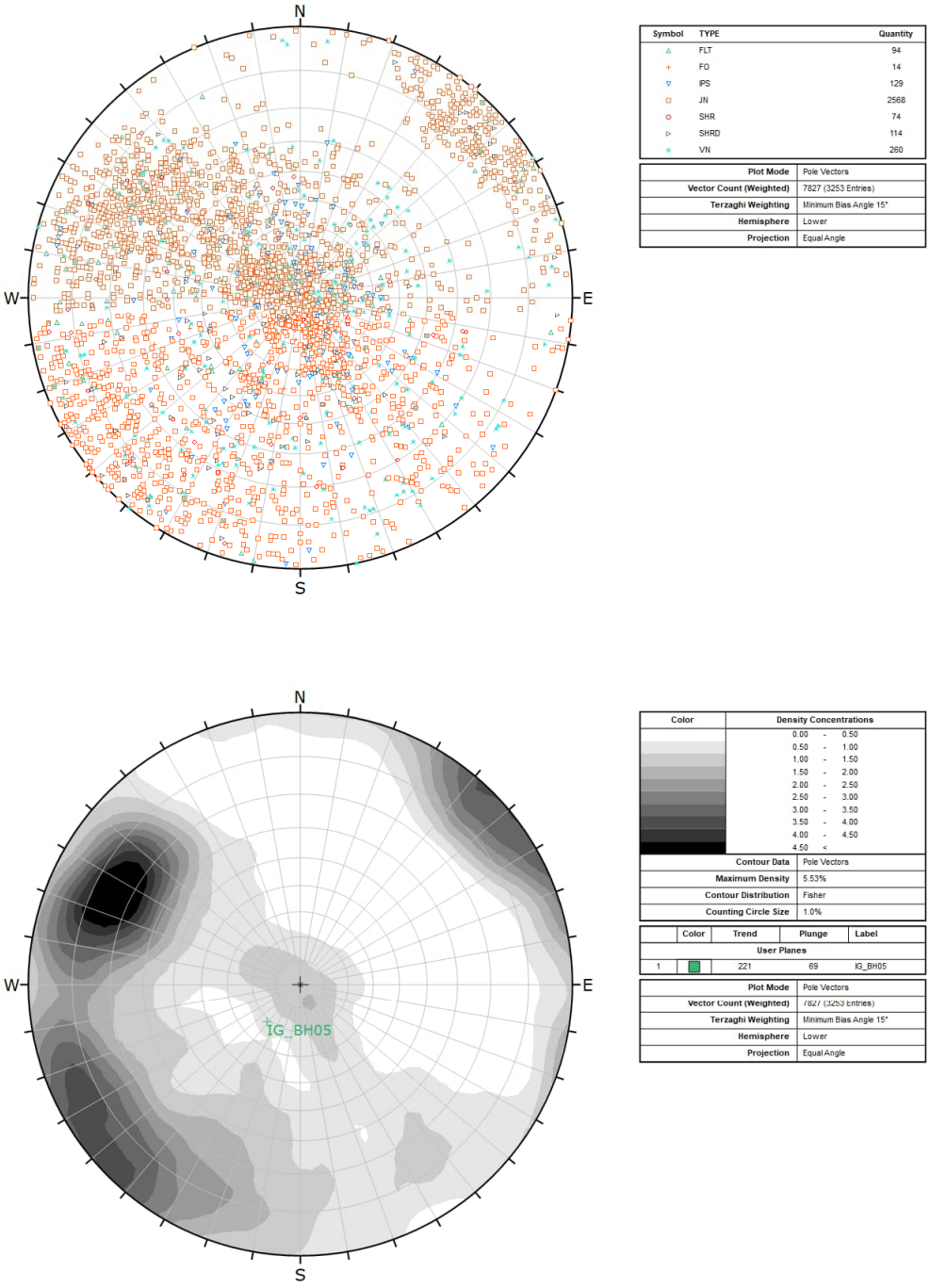


Figure 4: Stereographic Projection of all Integrated Structures for IG_BH05: Top: Structures by Type; Bottom: Contour Plot (with Terzaghi Weighting)

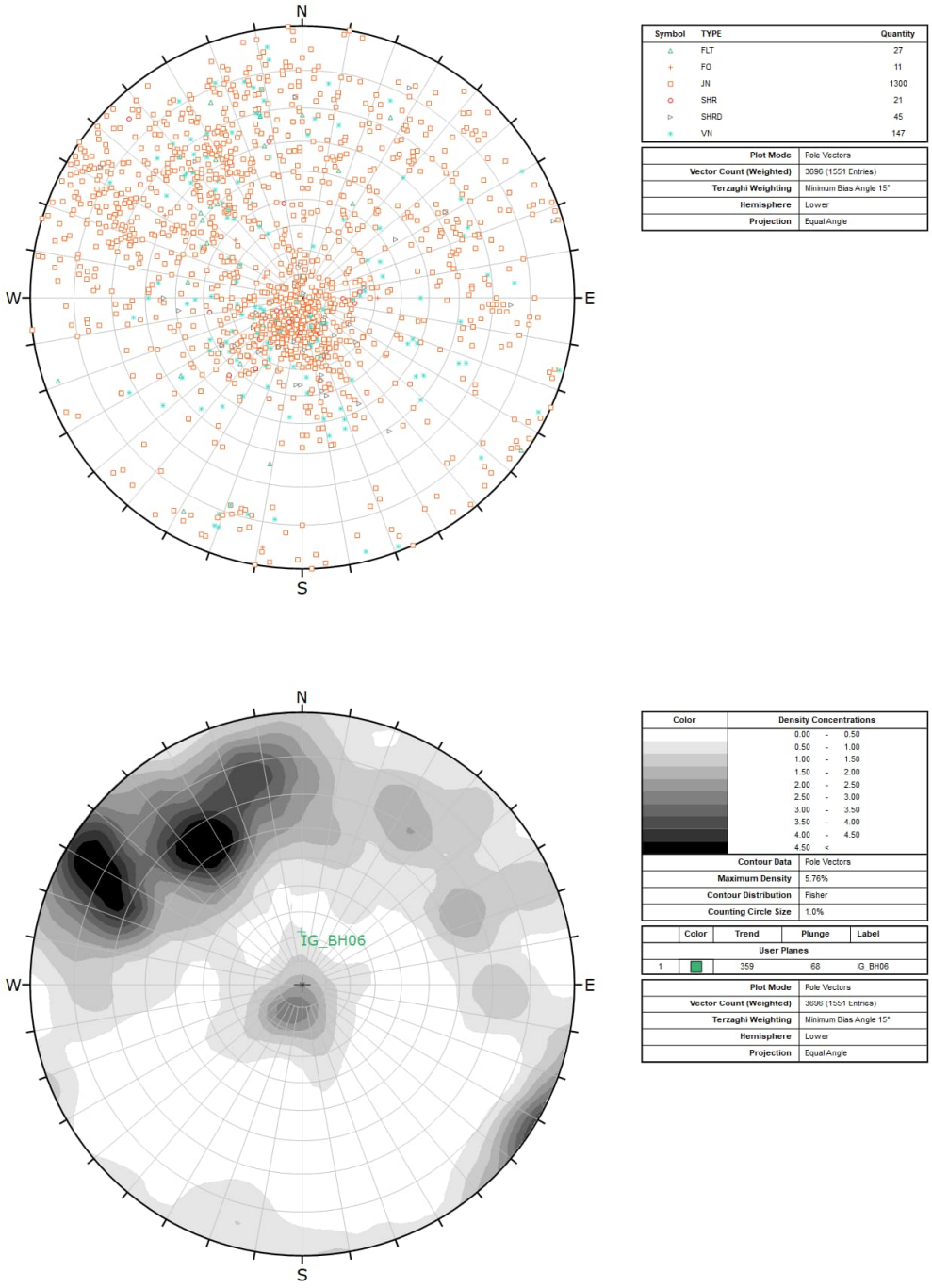


Figure 5: Stereographic Projection of all Integrated Structures for IG_BH06: Top: Structures by Type; Bottom: Contour Plot (with Terzaghi Weighting)

5.0 GEOMECHANICS CLASSIFICATION, ROCK MASS RATING (RMR) INDEX

One of the widely used rock mass classifications is the Rock Mass Rating (RMR) system of Bieniawski (1973, 1976, and 1989). The classification includes information on the strength of the intact rock material, Rock Quality Designation (RQD), the spacing and surface properties of the structural discontinuities as well as ratings for the influence of subsurface groundwater and an adjustment for discontinuity orientation relative to the orientation of an engineered structure (e.g., tunnel). This classification was developed primarily for the estimation of the support requirements in tunnels, but its use has been expanded to cover many other fields (Hoek, 2018).

The RMR Index described herein is based on the RMR'89 classification. However, it incorporates information from only five of six characteristics: strength of the intact rock material, the spacing and/or number of fractures, the surface properties of the fractures, as well as ratings for the influence of subsurface groundwater, where interpreted to be present. Because of the unknown orientation of potential excavations, no adjustment can be made for the discontinuity orientations at this time. The RMR index therefore describes the rock mass independent of orientation and adjustments will have to be made when utilizing it for tunnel or shaft support estimations. For tunnels and shafts, the RMR = RMR Index - (0 to 12) points when accounting for orientation.

The RMR Index is therefore based on the sum of the following five ratings:

R_1 – Strength of intact rock material (Max rating = 15) – Based on laboratory testing (UCS); Strength Index values obtained during core logging using a series of tests (knife peeling, knife cutting, hammer pick, hammer blow) based on the Field Hardness Estimation tests as defined by the International Society for Rock Mechanics or ISRM Standards (1981). The strength index values correlate well with the UCS values;
R_2 – Drill core quality RQD (%) (Max rating = 20) – Compiled from core logging by run which is based on the ratio of the total length of core pieces between natural discontinuities that are longer than 10 cm to the core run length;
R_3 – Spacing of discontinuities (Max rating = 20) – Compiled from core logging by run and presented in the Final Structure Log;
R_4 – Condition of discontinuities (Max rating = 30) – Compiled from core logging for each individual fracture, compiled by run and presented in the Final Structure Log; the minimum value for the run was used in the estimation of RMR; and
R_5 – Groundwater condition (Max rating = 15) – Compiled from hydraulically conductive features (HCF) identified during hydrogeological testing (20 m long straddle packer tool) of the borehole and supported by Flowing Fluid Electrical Conductivity (FFEC) logs.

A description of the ratings based on the above five parameters can be found in Table 2. Appendix A of the WP03 Data Reports for IG_BH05 and IG_BH06 (WSP 2023a, 2023b) and IG_BH04 (Wood, 2021) provide more detailed descriptions of the condition of discontinuities (therein referred to as Joint Condition Rating or JCR), compared to the original RMR'89 table, and were tailored for this project. When assigning the RMR Index rating for UCS, RQD and Spacing parameters, interpolations were carried out between defined rating categories. When assigning the RMR Index rating for the Groundwater condition parameter to areas coincident with HCFs, the general condition of 'Damp' was applied (R_5 = 10).

Table 2: Rock Mass Rating System (Geomechanics Classification of Rock Masses, Bieniawski (1989))

Parameter			Ranges of Values						
1	Strength of intact rock material	Point-load strength index (MPa)	>10	4 – 10	2 – 4	1 – 2	For this low range, uniaxial compressive test is preferred		
		Uniaxial compressive strength (MPa)	>250	100 – 250	50 – 100	25 – 50	5 – 25	1 – 5	<1
	Rating		15	12	7	4	2	1	0
2	Drill core quality RQD (%)		90 – 100	75 – 90	50 – 75	25 – 50	<25		
	Rating		20	17	13	8	3		
3	Spacing of discontinuities		>2 m	0.6 – 2 m	200 – 600 mm	60 – 200 mm	<60 mm		
	Ratings		20	15	10	8	5		
4	Condition of discontinuities		Very rough surfaces Not continuous No separation Unweathered wall rock	Slightly rough surfaces Separation < 1 mm Slightly weathered walls	Slightly rough surfaces Separation < 1 mm Highly weathered walls	Slickensided surfaces or Gouge < 5 mm thick or Separation 1 – 5 mm Continuous	Soft gouge > 5 mm thick or Separation > 5 mm Continuous		
	Rating		30	25	20	10	0		
5	Groundwater condition	Inflow per 10 m tunnel length (L/min)	None	<10	10 – 25	25 – 125	>125		
		Ratio: Joint water pressure / Major principal stress	0	<0.1	0.1 – 0.2	0.2 – 0.5	>0.5		
		General conditions	Completely dry	Damp	Wet	Dripping	Flowing		
	Rating[1]		15	10	7	4	0		

[1] – based on analysis of hydraulic conductivity testing of an HQ borehole (96 mm)

6.0 SUMMARY OF ROCK MASS CLASSIFICATION PARAMETERS

The identified parameters used to determine rock mass classification were measured directly in the field, and based on integration of some field information, including development of final structure log and determination of hydraulically conductive features. Both field measurements and laboratory testing data were utilized for the strength factor in this system. The parameters used to develop the rock mass classification, are based on the data presented in the following documents:

- acQuire core logging database including the WP03 core run data, WP03 rock strength index data, hydraulically conductive features (HCF) data (WP03-WP05-WP07 Integrated dataset), WP10 final structure log data (WP03-WP05 Integrated dataset), WP10 rock interval (lithology) data of IG_BH04, IG_BH05 and IG_BH06
- WP03 Data Report – Geological and Geotechnical Core Logging, Photography and Sampling for IG_BH04 (Wood, 2021), IG_BH05 (WSP, 2023a) and IG_BH06 (WSP, 2023b)
- WP04b Data Report – Geomechanical Testing of Core for IG_BH04 (WSP, 2023e), IG_BH05 (WSP, 2023f) and IG_BH06 (WSP, 2023g) – in preparation
- WP05 Data Report – Geophysical Well Logging for IG_BH04 (WSP, 2022a), IG_BH05 (WSP, 2023c) and IG_BH06 (WSP, 2023d)
- WP07 Data Report – Opportunistic Groundwater Sampling for IG_BH04 (WSP, 2023h), IG_BH05 (WSP, 2023i) and IG_BH06 (WSP, 2023j)
- WP10 Geological Integration reports for IG_BH04 (DesRoches et al. 2023), IG_BH05 (Markovic et al. 2024a) and IG_BH06 (Markovic et al. 2024b).

The following subsections provide a summary of the input to the RMR Index presented below for the five ratings listed above in Section 5.0.

6.1 Strength

6.1.1 IG_BH04

Discrete field strength index measurements (332) were only taken opportunistically while breaking the core with a geological hammer strike when sampling or fitting core into the core boxes. In general, the rock is classified as very strong rock (R5 – 64% of the data) with 32% of the readings as strong rock (R4) throughout the borehole. Eleven measurements were recorded as medium strong rock (R3).

This agrees with the results of the laboratory tests on samples collected during drilling, which reported an average UCS value of 216 MPa for biotite granodiorite tonalite based on 6 tests, 214 MPa for feldspar-phyric dykes based on 2 tests, and 240 MPa for feldspar-phyric biotite granodiorite-tonalite based on one test (WSP, 2023e; see also Table 3). Only one amphibolite sample was tested, which failed prematurely.

6.1.2 IG_BH05

Discrete field strength index measurements (331) were only taken opportunistically while breaking the core with a geological hammer strike when sampling or fitting core into the core boxes. In general, the rock is classified as very strong rock (R5 – 61% of the data) with 37% of the readings as extremely strong rock (R6) throughout the borehole. Eight measurements were recorded as strong rock (R4). There is an increased relative amount of R4 values in the upper half of the borehole and R6 dominating in the last 200 metres of the borehole.

This agrees with the results of the laboratory tests on samples collected during drilling, which reported an average UCS value of 210 MPa for biotite granodiorite tonalite based on 7 tests, and 275 MPa for diabase dykes based on 2 tests (WSP, 2023f; see also Table 3). Only one amphibolite sample of the two tested failed through intact rock, with a reported value of 234 MPa.

6.1.3 IG_BH06

Discrete field strength index measurements (306) were only taken opportunistically while breaking the core with a geological hammer strike when sampling or fitting core into the core boxes. In general, the rock is classified as very strong rock (R5 – 92% of the data) with 5% of the readings as extremely strong rock (R6) throughout the borehole. Seven measurements were recorded as strong rock (R4). There is an increased relative amount of R4 values between 470 m and 635 m depth of the borehole and R6 dominating above 90 m depth and below 590 m depth along the borehole. The amphibolite (3 occurrences), the biotite granodiorite tonalite (1 occurrence), and the feldspar-phyric tonalite dykes (1 occurrence) were all classified as very strong rock (R5).

This agrees with the results of the laboratory tests on samples collected during drilling, which reported an average UCS value of 218 MPa for biotite granodiorite tonalite based on 6 tests, and 277 MPa for feldspar-phyric tonalite dyke based on a single test (WSP, 2023g; see also Table 3). Only one amphibolite sample of the two tested failed through intact rock, with a reported value of 238 MPa.

Table 3: UCS Values and Locations of Samples for IG_BH04, IG_BH05 and IG_BH06

Borehole	Sample ID	Sample from Depth (m)	Sample to Depth (m)	Rock type	UCS (MPa)
IG_BH04	IG_BH04_UC001	447.33	447.47	Biotite granodiorite-tonalite	215
	IG_BH04_UC002	480.7	480.84	Biotite granodiorite-tonalite	228
	IG_BH04_UC003	510.53	510.67	Biotite granodiorite-tonalite	202
	IG_BH04_UC004	552.95	553.09	Biotite granodiorite-tonalite	211
	IG_BH04_UC005	617.44	617.58	Amphibolite	108[1]
	IG_BH04_UC006	624.03	624.17	Biotite granodiorite-tonalite	207
	IG_BH04_UC007	691.54	691.68	Biotite granodiorite-tonalite	231
	IG_BH04_UC008	889.92	890.06	Feldspar-phyric biotite granodiorite-tonalite	240
	IG_BH04_UC009	435.27	435.41	Feldspar-phyric tonalite dyke	179[1]
	IG_BH04_UC010	741.19	741.33	Feldspar-phyric tonalite dyke	250
IG_BH05	IG_BH05_UC001	296.54	296.68	Diabase Dyke	278
	IG_BH05_UC002	315.55	315.69	Diabase Dyke	272
	IG_BH05_UC003	527.71	527.85	Biotite granodiorite-tonalite	192
	IG_BH05_UC004	588.72	588.86	Biotite granodiorite-tonalite	185
	IG_BH05_UC005	642.84	642.98	Biotite granodiorite-tonalite	210
	IG_BH05_UC006	703.35	703.49	Biotite granodiorite-tonalite	213
	IG_BH05_UC007	753.4	753.54	Biotite granodiorite-tonalite	235

Borehole	Sample ID	Sample from Depth (m)	Sample to Depth (m)	Rock type	UCS (MPa)
	IG_BH05_UC008	806.63	806.77	Biotite granodiorite-tonalite	210
	IG_BH05_UC009	853.06	853.2	Biotite granodiorite-tonalite	227
	IG_BH05_AR041	785.91	786.05	Amphibolite	234
	IG_BH05_AR053	857.24	857.38	Amphibolite	152[1]
IG_BH06	IG_BH06_UC001	559.27	559.41	Biotite granodiorite-tonalite	220
	IG_BH06_UC002	611.13	611.27	Biotite granodiorite-tonalite	201
	IG_BH06_UC003	672.3	672.44	Biotite granodiorite-tonalite	243
	IG_BH06_UC004	733.05	733.19	Biotite granodiorite-tonalite	209
	IG_BH06_UC005	792.67	792.81	Biotite granodiorite-tonalite	191
	IG_BH06_UC006	842.14	842.28	Biotite granodiorite-tonalite	244
	IG_BH06_AR015	465.94	466.08	Feldspar-phyric tonalite dyke	277
	IG_BH06_AR024	572.63	572.77	Amphibolite	186
	IG_BH06_AR047	811.38	811.52	Amphibolite	238

[1] – sample contained and failed along pre-existing structures.

6.2 RQD

6.2.1 IG_BH04

In general, the rock is considered to be excellent rock quality, averaging 97% RQD along the borehole. The minimum RQD value recorded is approximately 58%, with the exception of two core runs showing values less than 20%: 125 m (0%) and 327 m (18%). These lower values were associated with shear zones or broken core zones. When considering the core runs where dykes or amphibolite were encountered, RQD values are observed to be slightly reduced. This slight reduction is observed particularly when considering core runs within the amphibolite unit (Wood, 2021).

6.2.2 IG_BH05

The results for IG_BH05 indicate that overall, the rock quality is excellent, averaging 100% RQD, and ranging between 77% and 100%. The lowest RQDs are recorded near surface, in runs at approximately 167 m depth, and in runs that intersect an aplite dyke (WSP, 2023a).

6.2.3 IG_BH06

The results for IG_BH06 indicate that overall, the rock quality is excellent, averaging 100% RQD, and ranging between 83% and 100%. The lowest RQDs are recorded around 700 m depth (WSP, 2023b).

6.3 Fracture Spacing

6.3.1 IG_BH04

Overall, 3% of the core by length has broken structure spacing less than 0.5 m. The broken structure frequency is generally highest in the upper 120 m of the borehole. In general, the core runs containing lithological contacts have an increased broken structure count. Typically, throughout the core, broken structures occur at a frequency

of one to none per metre (93% of the core by length), with the highest fractures per metre observed between 98 m and 110 m.

For the intact structures, 29% of the core by length has an intact structure frequency of greater than 3 per metre. The highest logged intact structure frequencies can be found in the core runs from 572.21 m to 584.21 m. It is noted that most of the logged contacts in IG_BH04 were intact.

The true fracture spacing can only be estimated after all measured discontinuities are plotted on a stereonet and sets are identified. This usually results in spacings greater than the inverse of the fracture frequency from the logs.

6.3.2 IG_BH05

Typically, throughout the core, broken structures occur at a frequency of one to none per metre (93% of the core by length), especially below a borehole depth of 40 m, and between 715 m and 800 m. A broken structure frequency greater than two per metre was observed in 3% of the core by length. The highest logged broken structure count was 2.35 per metre, encountered at 717 m depth.

The broken structure frequency is highest in the upper half of the borehole. Along the length of the borehole, shorter zones of greater broken structure frequency are interspersed within zones of lesser broken fracture frequency. In general, the core runs containing lithological contacts have an increased broken structure count. However, it should be noted that feldspar-phyric tonalite dykes and pegmatite dykes are characterized by intact contacts and are not commonly associated with increased fracture frequency.

For the intact structures, 27% of the core by length has an intact structure frequency of greater than 3 per metre, with 11.8 per metre as the highest logged intact structure frequency. Typically, intact structures were recorded approximately once per metre. Alternating zones of greater and lesser frequency persist along the length of the borehole, following the broken structure frequency trends (WSP, 2023a).

6.3.3 IG_BH06

Throughout the core, broken structures, occur at a frequency of zero to 1.67 occurrences per metre. The core runs with broken structures are observed mostly above a borehole depth of 175 m, and below 625 m depth. A broken structure frequency greater than one per metre was observed in 0.9% of the core by length. The highest logged broken structure count was 1.67 per metre, encountered at 12 m depth.

In general, the core runs containing lithological contacts have an increased broken structure count. However, it should be noted that feldspar-phyric tonalite dykes and pegmatite dykes are characterized by intact contacts and are not commonly associated with increased fracture frequency.

For the intact structures, 10.9% of the core by length has an intact structure frequency of greater than 3 per metre. The highest logged intact structure frequency of 9.8 per metre, can be found in the core run from 724.90 m to 727.85 m. On average, intact structures were recorded approximately once per metre. Alternating zones of greater and lesser frequency persist along the length of the borehole, following the broken structure frequency trends (WSP, 2023b).

6.4 Condition of Discontinuities

6.4.1 IG_BH04

The condition of discontinuities was recorded in all core logging data for all fracture types (i.e., faults, joints, veins) as a Joint Condition Rating (JCR). It is a frictional index based on intactness, geological aperture, rock wall

strength, shape, roughness, infill character, and infill type of all fracture types (joints, faults and veins). Most of the logged broken joints (91%) exhibit zero geological aperture. In the remaining occurrences mm- to cm-scale geological apertures were logged. In general, clean structures and structures with quartz, calcite, feldspar, muscovite, biotite, and epidote infill show high JCR values. Iron oxide (hematite and limonite) as well as chlorite mineral infill yield slightly wider ranges of JCR, while the soft or slick mineral infills (clay, soft gouge, and broken rock) show lower JCR ratings.

A total of eight faults were logged in IG_BH04, six of which were broken, allowing the full plane to be observed. Five exhibited no geological aperture and the other three were mm- to cm-scale.

JCR values were generally higher than 15 with 92% of the structures being intact and having the maximum rating of 30 (Wood, 2020). The broken joints were assigned JCR values ranging between 9 and 30, the majority of which lie between 16 and 25. In general, features logged within the amphibolite have slightly reduced JCR values when compared to the overall data distribution.

The minimum JCR for the run was adopted when calculating the RMR for the run. A separate assessment with the average JCR for the run showed very little difference from the minimum JCR assessment.

6.4.2 IG_BH05

A total of 2594 joints were logged on core and in televiewer in IG_BH05 and their occurrences are distributed along the entire length of the borehole. 129 occurrences (5%) of the joints were observed to be broken, while the remaining 2465 (95%) joints were intact or partially intact. The latter were assigned JCR values of 30, while the broken joints were assigned JCR values ranging between 15 and 30, the majority of which lie between 19 and 25. The majority of the logged joints (82%) exhibited zero aperture. In the remaining occurrences mm- to cm-scale apertures were logged. Of the total logged joints, 51 were logged as clean (2%), elsewhere the surface condition was logged as stained, slightly altered, coated, or infilled.

A total of 94 faults were logged in IG_BH05. The fault occurrences are distributed along the entire length of the borehole (Figure 7). The main diagnostic criteria used to identify a fault in the recovered core was the presence of slickenlines on the fault surface. A small percentage of the logged faults (16%) were broken, allowing the full plane to be observed. For intact faults, the slickensided fault surface was observed when the core broke along the fault plane during handling or displacement of an adjacent structure was observed. Intact and partially intact faults received a JCR of 30, with the remainder having assigned JCR values ranging between 9 and 22.

In general, clean structures and structures with the following mineral infill show high JCR values (ranging from 12 and 30, with an average of 29): quartz, calcite, feldspar, muscovite, biotite, and iron oxide (hematite) infill. Lower JCR ratings are associated with soft or slick mineral infills (WP10 – Final Structure Log).

6.4.3 IG_BH06

A total of 1305 joints were logged in IG_BH06 and their occurrences are distributed along the entire length of the borehole. 38 occurrences (3%) of the joints were observed to be broken, while the remaining 1267 (97%) joints were intact or partially intact. The latter were assigned JCR values of 30, while the broken joints were assigned JCR values ranging between 15 and 27. Approximately half of the logged broken joints (53%) have zero aperture. In the remaining occurrences mm- to cm-scale apertures were logged. Of the total logged joints, 17 were logged as clean (1%), 183 have no information about infill character (14%), and, elsewhere, the surface condition was logged as stained, slightly altered, coated, or infilled.

A total of 27 faults were logged in IG_BH06. The fault occurrences are observed mainly in the upper 82 m along the borehole and between 425 m and 510 m depth, with few occurrences at greater depth (Figure 8). The main diagnostic criteria used to identify a fault in the recovered core was the presence of slickenlines on the fault surface. A small percentage of the logged faults (18.5%) were broken, allowing the full plane to be observed. For intact faults, the slickensided fault surface was observed when the core broke along the fault plane during handling or when displacement of an adjacent structure was observed. All intact and partially intact faults had a JCR of 30, and the broken faults had JCR values ranging between 8 and 18.

In general, clean structures and structures with the following mineral infill show high JCR values (ranging from 12 and 30, with an average of 29): quartz, calcite, feldspar, muscovite, biotite, and iron oxide (hematite) infill. Lower JCR ratings are associated with soft or slick mineral infills (stiff gouge, average JCR = 8) (WP10 – Final Structure Log).

6.5 Groundwater

Intervals with groundwater were identified as hydraulically conductive features (HCFs) by either correspondence to the location of an opportunistic water sample (OGW), or to an interpreted inflow during flowing fluid electrical conductivity (FFEC) logging.

6.5.1 IG_BH04

A total of eleven (11) HCF intervals were identified in IG_BH04 (Table 4). All core runs that overlap with locations of HCF intervals are assigned a rating of 10 (out of 15) indicating ‘damp’ conditions. The remainder of the core runs along the borehole are assigned a rating of 15 indicating ‘dry’ conditions.

Table 4: Summary of Hydraulically Conductive Feature Intervals for IG_BH04

Borehole ID	HCF ID	From [m down hole]	To [m down hole]
IG_BH04	IG_BH04_HCF_1	113.2	114.2
IG_BH04	IG_BH04_HCF_5	477.7	497.73
IG_BH04	IG_BH04_HCF_2	580.4	581.4
IG_BH04	IG_BH04_HCF_3	616	617
IG_BH04	IG_BH04_HCF_4	620.1	621.1
IG_BH04	IG_BH04_HCF_6	625.11	645.14
IG_BH04	IG_BH04_HCF_7	683.64	703.67
IG_BH04	IG_BH04_HCF_8	849.93	869.96
IG_BH04	IG_BH04_HCF_9	902.64	922.67
IG_BH04	IG_BH04_HCF_10	938.5	958.53
IG_BH04	IG_BH04_HCF_11	959.65	1000.2

6.5.2 IG_BH05

A total of thirteen (13) HCF intervals were identified in IG_BH05 (Table 5). All core runs that overlap with locations of HCF intervals are assigned a rating of 10 (out of 15) indicating ‘damp’ conditions. The remainder of the core runs along the borehole are assigned a rating of 15 indicating ‘dry’ conditions.

Table 5: Summary of Hydraulically Conductive Feature Intervals for IG_BH05

Borehole ID	HCF ID	From [m down hole]	To [m down hole]
IG_BH05	IG_BH05_HCF_1	92.8	93.8
IG_BH05	IG_BH05_HCF_2	157.9	158.9
IG_BH05	IG_BH05_HCF_3	161.6	162.6
IG_BH05	IG_BH05_HCF_4	167.1	168.4
IG_BH05	IG_BH05_HCF_5	167.5	168.5
IG_BH05	IG_BH05_HCF_6	228.7	229.7
IG_BH05	IG_BH05_HCF_7	311.8	312.8
IG_BH05	IG_BH05_HCF_8	317.5	318.5
IG_BH05	IG_BH05_HCF_9	391.3	392.3
IG_BH05	IG_BH05_HCF_10	789.4	790.4
IG_BH05	IG_BH05_HCF_12	792.31	812.33
IG_BH05	IG_BH05_HCF_11	856.6	857.6
IG_BH05	IG_BH05_HCF_13	967	987.02

6.5.3 IG_BH06

A total of four (4) HCF intervals were identified in IG_BH06 (Table 6). All core runs that overlap with locations of HCF intervals are assigned a rating of 10 (out of 15) indicating ‘damp’ conditions. The remainder of the core runs along the borehole are assigned a rating of 15 indicating ‘dry’ conditions.

Table 6: Summary of Hydraulically Conductive Feature Intervals for IG_BH06

Borehole ID	HCF ID	From [m down hole]	To [m down hole]
IG_BH06	IG_BH06_HCF_1	152.47	153.47
IG_BH06	IG_BH06_HCF_2	696	716.03
IG_BH06	IG_BH06_HCF_3	716.01	736.04
IG_BH06	IG_BH06_HCF_4	904	924.03

7.0 SUMMARY OF ROCK MASS CLASSIFICATION BY RUN

The RMR Index described herein per core run is based on the RMR’89 classification. The data collected from boreholes IG_BH04, IG_BH05 and IG_BH06 were used to assemble the geotechnical information.

The information for the five parameters comprising RMR$'^{89}$ was compiled as follows:

R_1 – Based on laboratory testing (UCS) and Strength Index values;

R_2 – RQD – Compiled from core logging by run;

R_3 – Spacing of discontinuities – Compiled by run from distances between fractures recorded from core logging;

R_4 – Condition of discontinuities– Available from core logging for each discontinuity individually; compiled by run using the minimum value for the run; and

R_5 – Groundwater condition – Compiled from hydraulically conductive features identified during hydrogeological testing of the borehole and supported by FFEC logs.

The RMR Index describes the rock mass characteristics independently of discontinuity orientations. An additional adjustment should be applied once the engineering application is known.

Figure 6 through Figure 8 show a summary of rock mass characteristics, including the components of RMR'^{89}, and the RMR Index profile by run along the borehole for boreholes IG_BH04, IG_BH05 and IG_BH06, respectively.

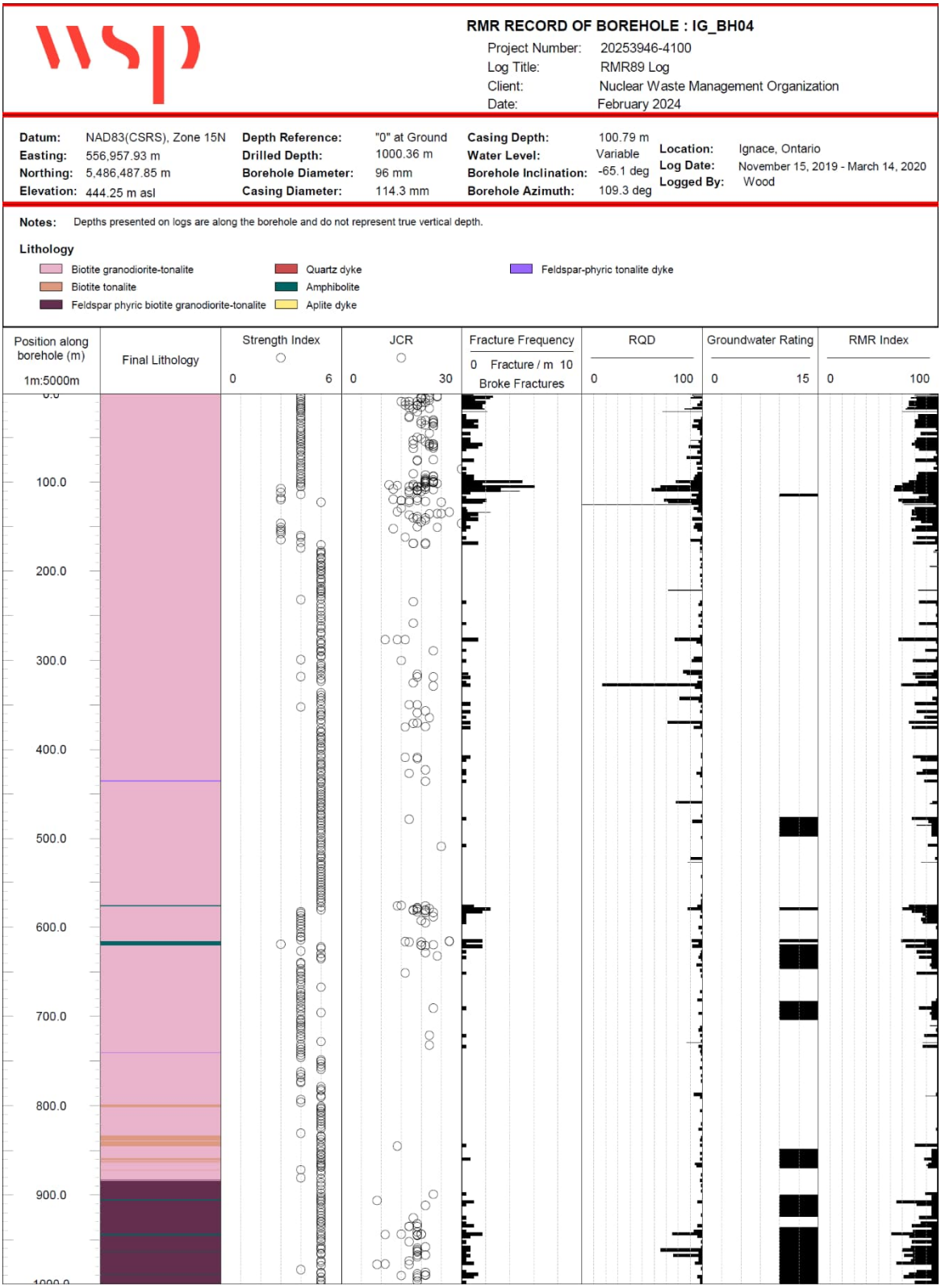


Figure 6: Summary Profile of Rock Mass Characteristics, Including Components of RMR'89, Used to Develop the RMR Index (Rightmost Column) for IG_BH04

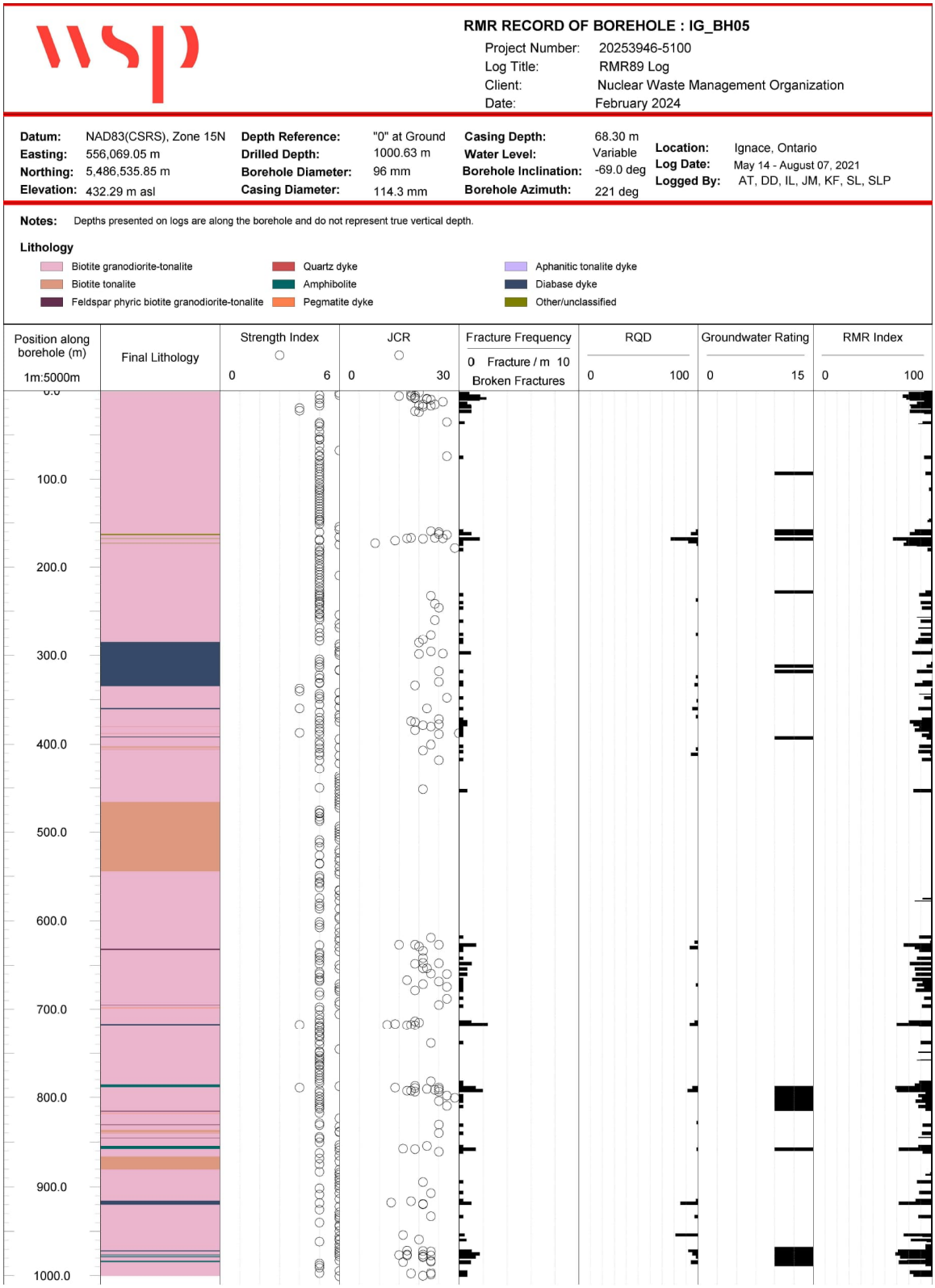


Figure 7: Summary Profile of Rock Mass Characteristics, Including Components of RMR'89, Used to Develop the RMR Index (Rightmost Column) for IG_BH05

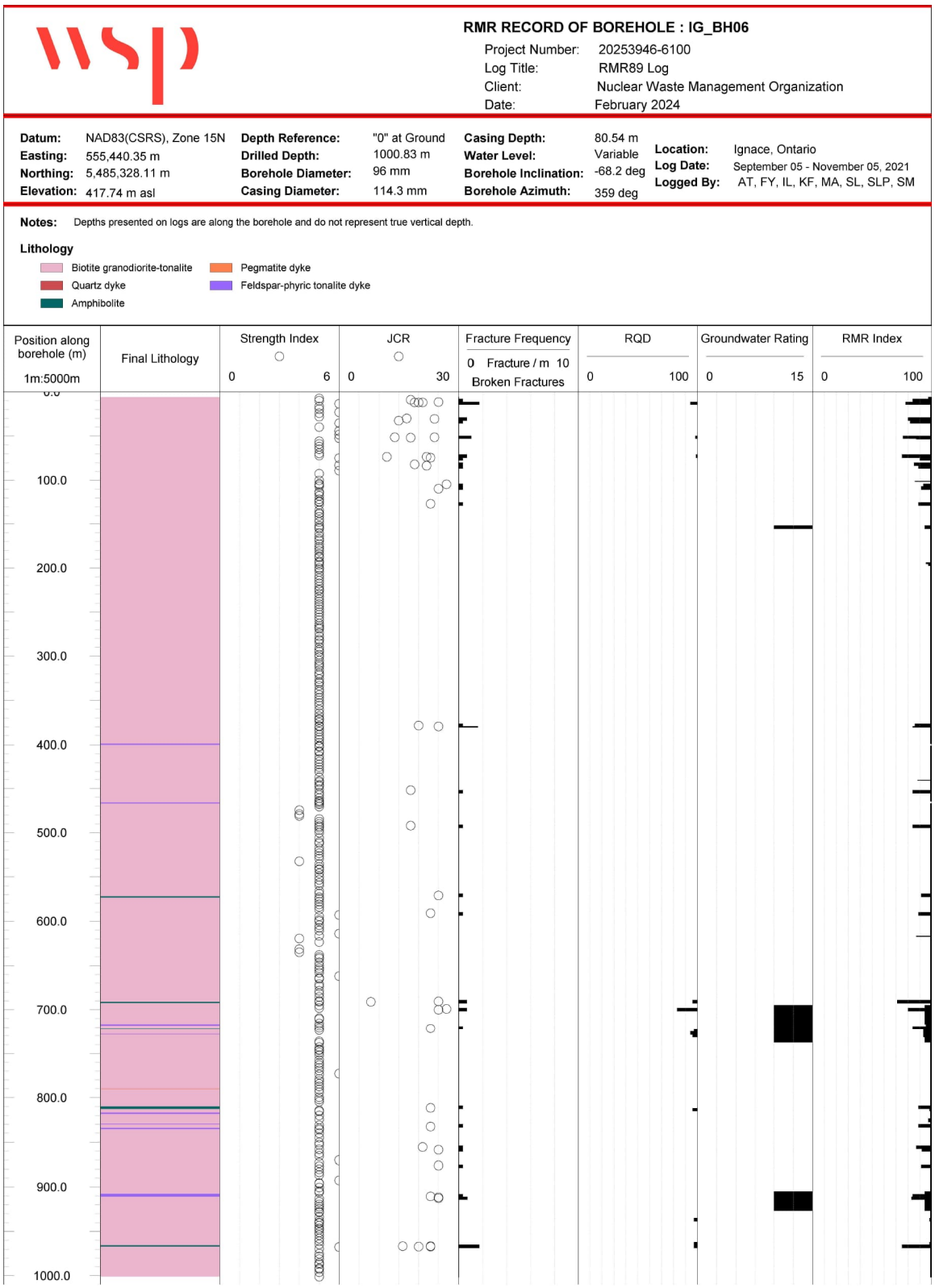


Figure 8: Summary Profile of Rock Mass Characteristics, Including Components of RMR'89, Used to Develop the RMR Index (Rightmost Column) for IG_BH06

8.0 SUMMARY OF ROCK MASS RATING INDEX DISTRIBUTION BY SECTIONS OF BOREHOLE IG_BH04, IG_BH05, AND IG_BH06

Distributions of the RMR Index for 100 m sections along the boreholes were based on the RMR'89 classification (see Figure 9 through Figure 11). This presentation of the data by borehole section in the form of histograms was made to allow an assessment of the variability of the rock quality with depth along borehole. Mean and median values for RMR Index for each 100 m section are presented in Table 7.

Table 7: Summary of Mean and Median Values for RMR Index for IG_BH04, IG_BH05 and IG_BH06

Depth (along hole) Interval	RMR Index for IG_BH04			RMR Index for IG_BH05			RMR Index for IG_BH06		
(m)	min	mean	median	min	mean	median	min	mean	median
0 – 100	70	86	82	75	94	99	75	94	99
100 – 200	63	86	88	67	95	99	86	98	99
200 – 300	67	96	99	83	96	99	99	99	99
300 – 400	69	93	99	81	95	99	84	98	99
400 – 500	78	95	99	84	98	99	84	98	99
500 – 600	70	95	99	85	98	99	89	98	99
600 – 700	69	93	94	76	93	99	71	98	99
700 – 800	87	97	99	69	94	99	80	96	99
800 – 900	80	97	99	72	95	99	87	97	99
900 – EOH*	61	83	82	69	91	95	75	97	99

* End of Hole: IG_BH04 EOH = 1000.36 m; IG_BH05 EOH = 1001.63 m; IG_BH06 EOH = 1000.83 m

8.1 Adjustments to RMR Data for Engineering Use

8.1.1 Groundwater Ratings

The groundwater ratings used to generate the RMR Index profile were based on analysis of field hydrogeological testing of 20 m intervals in the more conductive features of each borehole, as identified from core logging and FFEC testing. The hydraulic conductivity values that led to the identification of the more conductive zones are representative only for the size of the HQ borehole (96 mm).

When using these data for engineering analysis or design of larger excavations, e.g., tunnels or shafts, a re-assessment of the groundwater conditions will be required to replace the ratings provided in this report.

8.1.2 Rating Adjustments for Discontinuity Orientations

The RMR Index ratings presented in this report will need to be adjusted by an additional parameter, namely, the influence of the orientation of the discontinuities. This step is usually left to the user of the data because the influence of the discontinuity orientations depends on the engineering application (see Table 8 and Table 9).

Table 8: Rating Adjustment for Discontinuity Orientations (see also Table 9)

Strike and Dip Orientations of Discontinuities		Very Favourable	Favourable	Fair	Unfavourable	Very Unfavourable
Ratings	Tunnels and mines	0	-2	-5	-10	-12
	Foundations	0	-2	-7	-25	-25
	Slopes	0	-5	-25	-50	-60

Table 9: Effect of Discontinuity Strike and Dip on Orientation in Tunnelling

Strike perpendicular to tunnel axis		Strike parallel to tunnel axis	
Drive with dip - Dip 45 – 90°	Drive with dip - Dip 20 – 45°	Dip 45 – 90°	Dip 20 – 45°
Very favourable	Very favourable	Very unfavourable	Fair
Drive against dip - Dip 45-90°	Drive against dip - Dip 20-45°	Dip 0-20° - Irrespective of strike	
Fair	Unfavourable	Fair	

Modified after Wickham et al (1972)

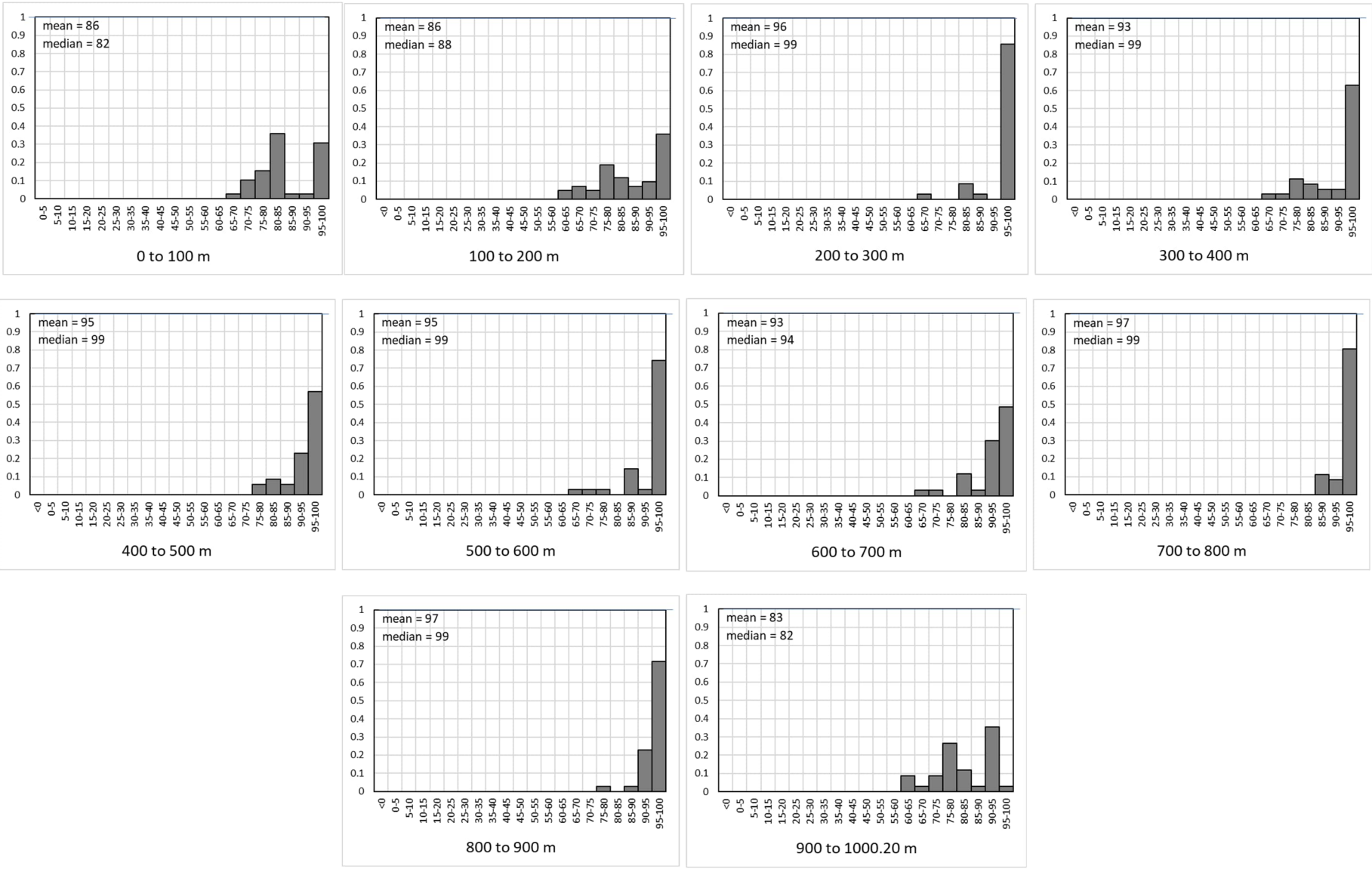


Figure 9: RMR Index Distribution for 100 m Sections of Borehole (RMR Index by Run) for IG_BH04

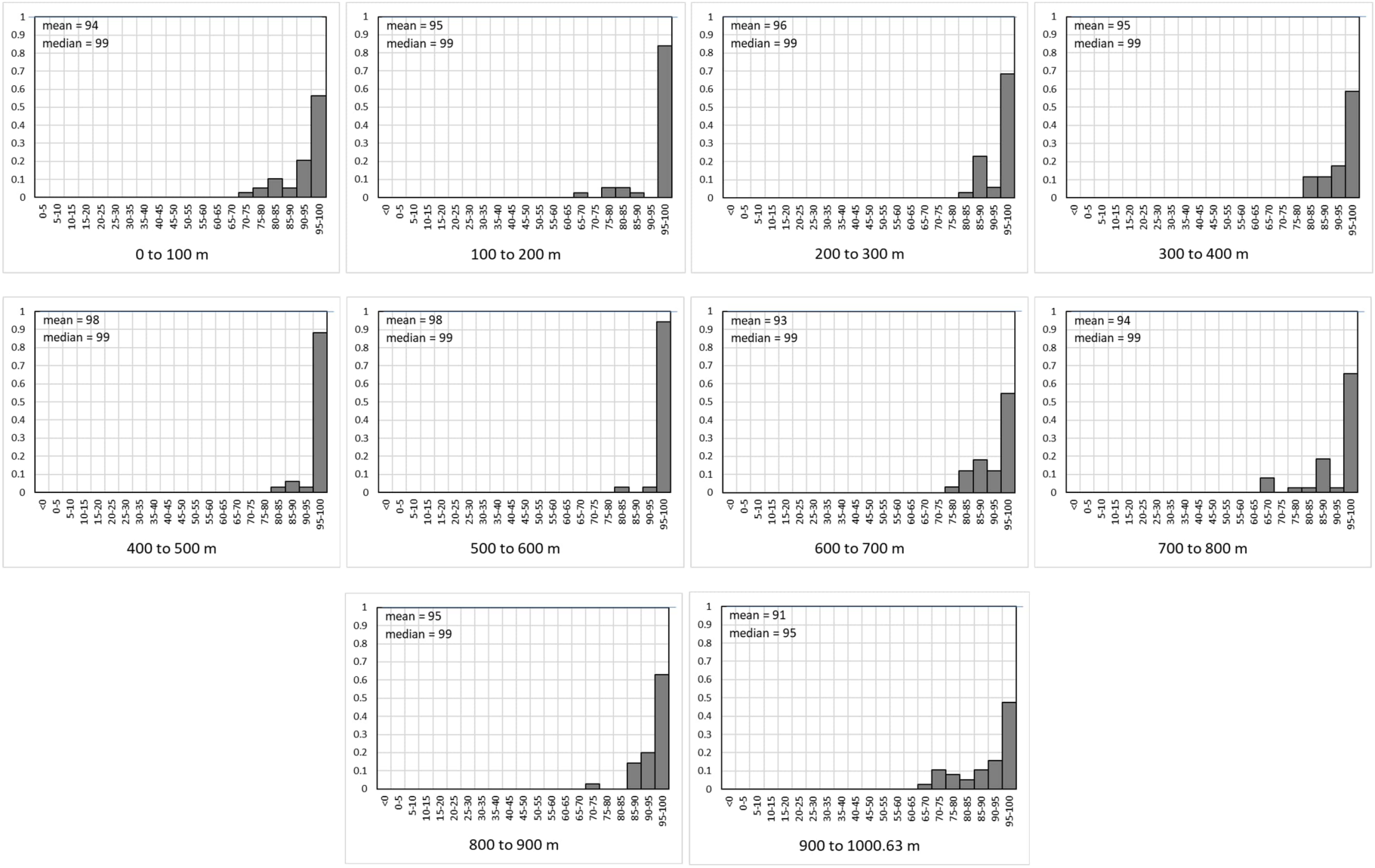


Figure 10: RMR Index Distribution for 100 m Sections of Borehole (RMR Index by Run) for IG_BH05

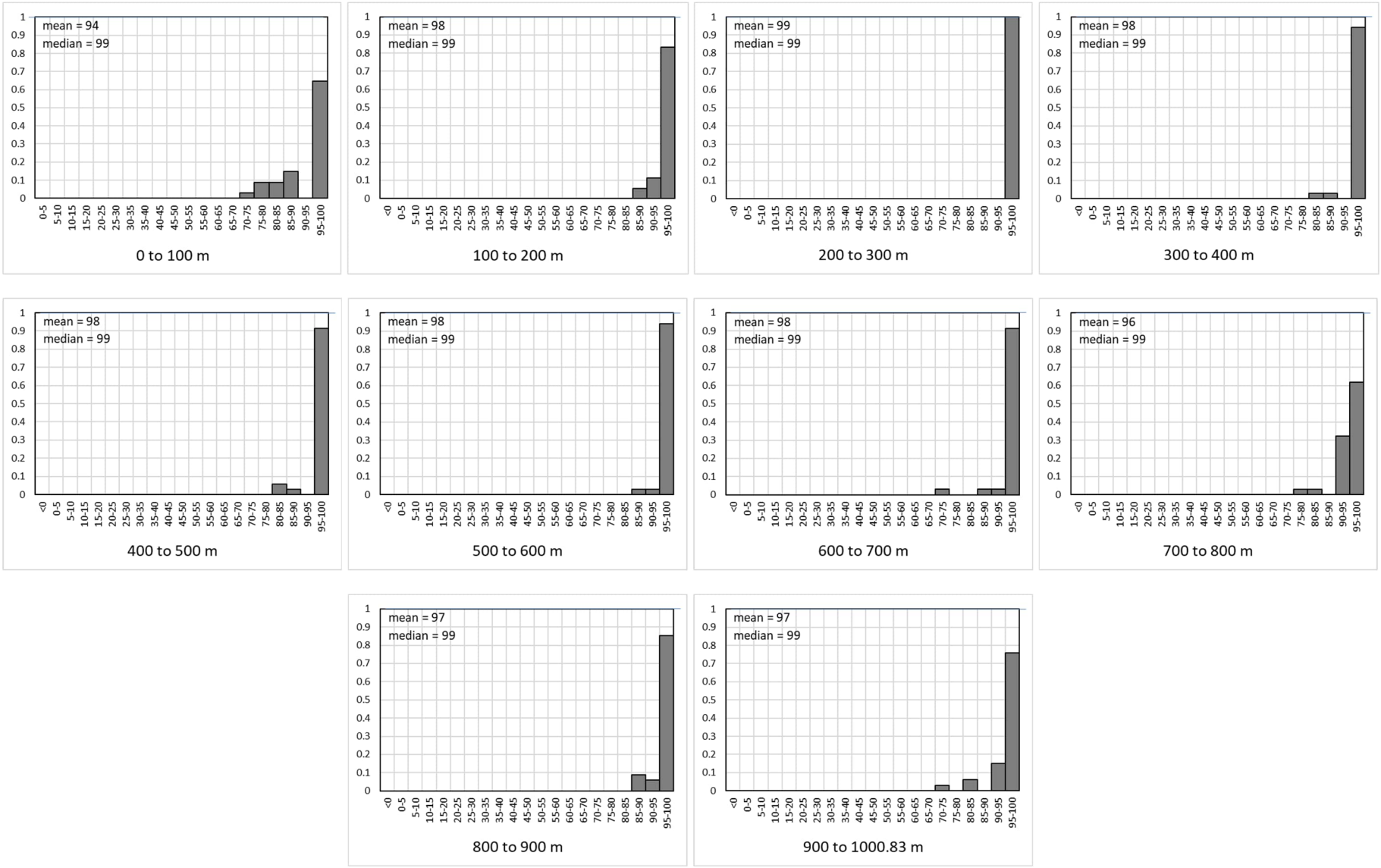


Figure 11: RMR Index Distribution for 100 m Sections of Borehole (RMR Index by Run) for IG_BH06

9.0 REFERENCES

Blackburn, C.E. and Hinz, P., 1996. Gold and base metal potential of the northwest part of the Raleigh Lake greenstone belt, northwestern Ontario-Kenora Resident Geologist's District; in Summary of Field Work and Other Activities 1996, Ontario Geological Survey, Miscellaneous Paper 166, p.113-115.

Bieniawski, Z.T. 1973. Engineering classification of jointed rock masses. Trans S. Afr. Inst. Civ. Engrs 15, 335-344.

Bieniawski, Z.T. 1976. Rock mass classification in rock engineering. In Exploration for rock engineering, proc. of the symp., (ed. Z.T. Bieniawski) 1, 97-106. Cape Town: Balkema.

Bieniawski, Z.T. 1989. Engineering rock mass classifications. New York: Wiley.

DesRoches, A., Sykes, M., Parmenter, A. and Sykes, E., 2018. Lineament Interpretation of the Revell Batholith and Surrounding Greenstone Belts (Nuclear Waste Management Organization. No. NWMO-TR-2018-19).

DesRoches, A., A. Parmenter and S. Markovic. 2023. Phase 2 Initial Borehole Drilling and Testing, Ignace Area WP10 - Geological Integration Report for Borehole IG_BH04. NWMO Report APM-REP-01332-0372. Toronto.

Golder (Golder Associates Ltd.) and PGW (Paterson, Grant and Watson Ltd.), 2017b. Detailed Geological Mapping – Ignace Ontario – APM Phase 2 Assessment. Prepared for Nuclear Waste Management Organization (NWMO). NWMO Report Number: APM-REP-01332-0225.

Hoek, E. 2018. Practical Rock Engineering (2018 ed.). https://www.rocscience.com.

ISRM, 1981. Rock characterization Testing and Monitoring - ISRM Suggested Methods. Pergamon Press, London, England, p.32, ed. Brown, E.T.

Markovic, S., A. DesRoches and A. Parmenter. 2024a. Phase 2 Initial Borehole Drilling and Testing, Ignace Area WP10 - Geological Integration Report for Borehole IG_BH05. NWMO Report APM-REP-01332-0397. Toronto.

Markovic, S., A. DesRoches and L. Debono. 2024b. Phase 2 Initial Borehole Drilling and Testing, Ignace Area WP10 - Geological Integration Report for Borehole IG_BH06. NWMO Report APM-REP-01332-0399. Toronto.

OGS (Ontario Geological Survey), 2011. 1:250 000 scale bedrock geology of Ontario, Ontario Geological Survey, Miscellaneous Release Data 126 - Revision 1.

Parmenter, A., Waffle, L. and DesRoches, A., 2020. An updated bedrock geology map and geological database for the northern portion of the Revell batholith (No. NWMO-TR-2020-08). Nuclear Waste Management Organization.

SGL (Sander Geophysics Limited), 2015. Phase 2 Geoscientific Preliminary Assessment, Acquisition, Processing and Interpretation of High-Resolution Airborne Geophysical Data, Township of Ignace, Ontario. Prepared for Nuclear Waste Management Organization (NWMO). NWMO Report Number: APM-REP-06145-0002.

SRK (SRK Consulting, Inc.) and Golder, 2015. Phase 2 Geoscientific Preliminary Assessment, Observation of General Geological Features, Township of Ignace, Ontario. Prepared for Nuclear Waste Management Organization. NWMO Report Number: APM-REP-06145-0004.

Stone, D., 2009. Geology of the Bending Lake Area, Northwestern Ontario; in Summary of Field Work and Other Activities 2009. Ontario Geological Survey. Open File Report 6240.

Stone, D., 2010a. Geology of the Stormy Lake Area, Northwestern Ontario; in Summary of Field Work and Other Activities 2010. Ontario Geological Survey, Open File Report 6260.

Stone, D., 2010b. Precambrian geology of the central Wabigoon Subprovince area, northwestern Ontario. Ontario Geological Survey, Open File Report 5422.

Stone, D., Halle, J. and Chaloux, E., 1998. Geology of the Ignace and Pekagoning Lake Areas, Central Wabigoon Subprovince; in Summary of Field Work and Other Activities 1998, Ontario Geological Survey, Misc. Paper 169.

Stone, D., Davis, D.W., Hamilton, M.A. and Falcon, A., 2010. Interpretation of 2009 Geochronology in the Central Wabigoon Subprovince and Bending Lake Areas, Northwestern Ontario, in Summary of Field Work and Other Activities 2010, Ontario Geological Survey, Open File Report 6260.

Wickham, G.E., Tiedemann, H.R. and Skinner, E.H. 1972. Support determination based on geologic predictions. In Proc. North American rapid excav. tunneling conf., Chicago, (eds K.S. Lane and L.A. Garfield), 43-64. New York: Soc. Min. Engrs, Am. Inst. Min. Metall. Petrolm Engrs.

Wood, 2021. Phase 2 Initial Borehole Drilling and Testing, Ignace Area. WP03 Data Report – Geological and Geotechnical Core Logging, Photography and Sampling for IG_BH04. NWMO Report Number: APM-REP-01332-0258.

WSP, 2023a. Phase 2 Initial Borehole Drilling and Testing at IG_BH04/05/06 – Ignace Area. WP03 Data Report – Geological and Geotechnical Core Logging, Photography, and Sampling for IG_BH05. NWMO Report Number: APM-REP-01332-0382.

WSP, 2023b. Phase 2 Initial Borehole Drilling and Testing at IG_BH04/05/06 – Ignace Area. WP03 Data Report – Geological and Geotechnical Core Logging, Photography, and Sampling for IG_BH06. NWMO Report Number: APM-REP-01332-0283.

WSP, 2022a. Phase 2 Initial Borehole Drilling and Testing at IG_BH04/05/06 – Ignace Area. WP05 Data Report - Geophysical Well Logging for IG_BH04. NWMO Report Number: APM-REP-01332-0356.

WSP, 2023c. Phase 2 Initial Borehole Drilling and Testing at IG_BH04/05/06 – Ignace Area. WP05 Data Report - Geophysical Well Logging for IG_BH05. NWMO Report Number: APM-REP-01332-0366.

WSP, 2023d. Phase 2 Initial Borehole Drilling and Testing at IG_BH04/05/06 – Ignace Area. WP05 Data Report - Geophysical Well Logging for IG_BH06. NWMO Report Number: APM-REP-01332-0367.

WSP, 2023e. Phase 2 Initial Borehole Drilling and Testing, Ignace Area. WP04B Data Report – Geomechanical Testing of Core for IG_BH04. NWMO Report Number: APM-REP-01332-0458.

WSP, 2023f. Phase 2 Initial Borehole Drilling and Testing, Ignace Area. WP04B Data Report – Laboratory Geomechanical Test of Core IG_BH05. NWMO Report Number: APM-REP-01332-0389.

WSP, 2023g. Phase 2 Initial Borehole Drilling and Testing, Ignace Area. WP04B Data Report – Laboratory Geomechanical Test of Core IG_BH06. NWMO Report Number: APM-REP-01332-0390.

WSP, 2023h. Phase 2 Initial Borehole Drilling and Testing at IG_BH04/05/06, Ignace Area. WP07 Data Report - Opportunistic Groundwater Sampling for IG_BH04. NWMO Report Number: APM-REP-01332-0281.

WSP, 2023i. Phase 2 Initial Borehole Drilling and Testing at IG_BH04/05/06, Ignace Area. WP07 Data Report - Opportunistic Groundwater Sampling for IG_BH05. NWMO Report Number: APM-REP-01332-0357.

WSP, 2023j. Phase 2 Initial Borehole Drilling and Testing at IG_BH04/05/06, Ignace Area. WP07 Data Report - Opportunistic Groundwater Sampling for IG_BH06. NWMO Report Number: APM-REP-01332-0358.



wsp.com